Throughput Optimization in Ambient Backscatter-Based Energy Constraint Cognitive Radio Networks

Syed Tariq Shah*, Maheen Fazal†, Mahmoud A. Shawky ‡, Rana M. Sohaib§, Syed Faraz Hasan‡, M. Ali Imran‡, Qammer H. Abbasi ‡

*School of Computer Science & Electronic Engineering, University of Essex, Colchester, UK
Email: Syed.shah@essex.ac.uk

† Telecommunication Engineering, Balochistan University of IT, Engineering & Management Sciences, Pakistan

§Directorate of Research Services, University of New England, Australia
Email: Faraz.Hasan@une.edu.au

‡James Watt School of Engineering, University of Glasgow, Glasgow, UK
Emails: {Mahmoud.Shawky, RanaMuhammad.Sohaib, Qammer.Abbasi, Muhammad.Imran}@glasgow.ac.uk

***Abstract*—Efficient utilisation of scarce resources, mainly radio and power, are the key research issues in the future Internet of Things (IoT) networks. This paper proposes an ambient energy harvesting and backscatter-enabled, energy-constrained cognitive IoT network. In our proposed scheme, the nodes in the secondary network efficiently utilise the primary network. More specifically, depending on the communication states (i.e. between busy or idle) of the primary network, the secondary nodes chose to operate either in energy harvesting mode (EHM), backscattering mode (BSM), or radio-frequency transmission mode (RFM). Furthermore, to maximise the sum-throughput of the secondary network, an optimisation problem is formulated and solved. The simulation results show that the proposed scheme outperforms the existing scheme regarding network sum-throughput.**

***Index Terms*—IoT, RF energy harvesting, ambient backscattering, cognitive IoT networks.**

I. Introduction

Internet-of-Things (IoT) basically refers to small physical devices that wirelessly communicate or exchange information and are connected to the internet. With the growing applications of IoT, it is anticipated that more than 50 billion IoT devices will be connected to the internet by 2025 [1], [2]. Because of their small and compact size, these IoT devices have limited battery life and are highly energy-constrained. In practice, replacing their batteries is either impossible or cost-ineffective, which yields an overall constrained network lifetime. Hence, to prolong the network lifetime, one of the convenient options is to utilise the ambient radio and power resources from the environment by exploiting wireless energy harvesting (WEH) and ambient backscatter (ABS) technologies [3], [4].

In WEH technology, ambient radio frequencies (RF) available in the surroundings are harvested to recharge the IoT devices [5]. However, in the case of ABS communication, the transmitter in ABS switches its mode between reflecting and non-reflecting modes to transmit bits "1" and "0", respectively. At the receiving end, envelope detection and averaging techniques are used to decode the received backscattered information [4]. Both WEH and ABS communication technologies can simultaneously be used in a cognitive radio environment, where secondary network nodes (SNs) opportunistically utilise the radio and power resources of the primary network (PN) for both powering up its battery and information transmission [6]–[10]. More specifically, in WEH and ABS communication-enabled cognitive radio networks (CRN), the SNs can either adopt RF energy harvesting mode (EHM) or ABS communication mode (BSM) during the PN's busy period. Likewise, during the idle period, the SNs use the PN's idle radio resources and perform radio communication by utilising the energy harvested in the busy period.

An RF-powered cognitive radio network (CRN) with ABS communication capabilities has been studied in [11]. A network throughput maximization problem is formulated to find the optimal time-sharing among multiple SNs. It has also been shown that an optimal trade-off point exists between energy harvesting (EH) time and backscattering time. Gong et al. [10] proposed a novel method for wireless power transfer (WPT) to secondary networks via beacon stations. In their proposed scheme, the secondary nodes used the stored energy for RF transmission, whereas the other nodes in the network cooperate as backscatter relay nodes to enhance the overall network performance. Furthermore, the overall network throughput was also maximised by optimising both the WPT and relay strategy to backscatter.

A decode and forward (DF) relay-based cognitive network with EH and ambient backscatter capabilities was proposed in [12]. The source node communicates with the destination node via an energy constraint relay in their proposed scheme. Besides relaying operation, the relay also cognitively performs ABS communication to transmit its information to a secondary node. The performance of the proposed scheme has been evaluated in terms of outage probability, energy efficiency(EE), and network sum-rate. In [13], the authors presented a hetero-

geneous IoT network that utilises an opportunistic backscatter communication medium access control (OBM) protocol. The proposed protocol improves the network's EH process and data transmission efficiency. The network's throughput and overall EE are enhanced by optimizing transmission probabilities and using different contention techniques to minimize collisions. A novel approach to enhancing the EE of full-duplex backscatter communications with multiple backscatter devices (BDs) by enabling EH from both the energy source and preceding BDs through energy recycling is proposed in [14]. A joint optimization of time scheduling, beamforming, and reflection coefficient adjustment is formulated and solved through Dinkelbach's method and an iterative algorithm. Their simulation results show improved performance compared to legacy schemes. In [15], the authors propose a novel approach to address the challenges of localizing and energy harvesting in dynamic RF environments for IoT networks using backscatter communication systems. By integrating a machine learning framework with K-Nearest Neighbors and Random Forest classifiers, they achieve over 99% precision in localization and demonstrate the feasibility of RF energy harvesting, ensuring the system's robustness and self-sustainability. The authors in [16] introduce a sustainable approach for enhancing the throughput and enabling wireless charging in underwater networks via simultaneous wireless information and power transfer (SWIPT) from an autonomous underwater vehicle (AUV). Addressing the environmental and operational challenges of the Internet of Underwater Things (IoUT), they employ a reinforcement learning (RL) model, formulated as a Markov decision process (MDP), to optimise AUV trajectories for maximum throughput and energy efficiency. Preliminary results in a bespoke 3-D RL MATLAB environment demonstrate a 207% increase in energy efficiency over conventional methods.

Unlike the above-mentioned papers, this paper focuses on a WEH and ABS communication-enabled cognitive IoT network. In our considered scheme, the SNs scavenge the primary network's ambient power and idle radio resources. Specifically, the secondary nodes operate in either radio-frequency transmission mode (RFM), energy harvesting mode (EHM), or backscattering mode (BSM), depending on the conditions of the primary network. Moreover, an optimisation problem is formulated and solved to maximise the overall secondary network throughput. The optimisation problem aims to find the optimal values for backscattering time and radio transmission time during busy and idle states of the primary network, respectively. The obtained results show that the proposed scheme significantly improves the overall network sum-rate and superiority over the existing schemes.

The remainder of this paper is structured as follows: Section II outlines the considered system model and proposed scheme, along with the requisite assumptions. Subsequently, the numerical results and findings are detailed in Section III, while Section IV concludes the paper with a summary of the findings and implications.

II. System Model and Proposed Scheme

We consider a CRN where two different networks, namely, a primary radio network and a secondary IoT network, exist. The primary network is assumed to operate in a licensed band, whereas the secondary IoT network opportunistically utilizes the ambient power and radio resources of the primary network. As depicted in Fig.1, the Primary network consists of a primary transmitter (PT) and multiple primary receivers (PRs). Likewise, the secondary IoT network is comprised of K secondary transceivers (SNs) and a secondary receiver (SR), also termed the gateway. The Rayleigh fading channel gains from PT-to-SN_k and SN_k-to-SR are respectively denoted by g_{ps_k} and h_{sg_k}, whereas $k \in \mathbb{K}$ and $\mathbb{K}= (1, 2, 3...K)$. Similarly, the distance from PT-to-SN_k and SN_k-to-SR are denoted by d_{ps_k} and d_{sg_k}, respectively.

The overall transmission time frame of the considered CRN is depicted in Fig.2. The idle and busy periods of the primary network are denoted by α and $(1-\alpha)$, respectively. It can be observed from Fig.2 that during the busy period of the primary network, the SNs either adopt the BSM or EHM. The backscattering time and normalized EH time of k^{th} SN are denoted by ζ_k and $(1-\alpha-\zeta_k)$, respectively. Likewise, when the primary network is idle, SNs either adopt the BSM or RFM. The data transmission time during the idle period for SN_k is represented by τ_k.

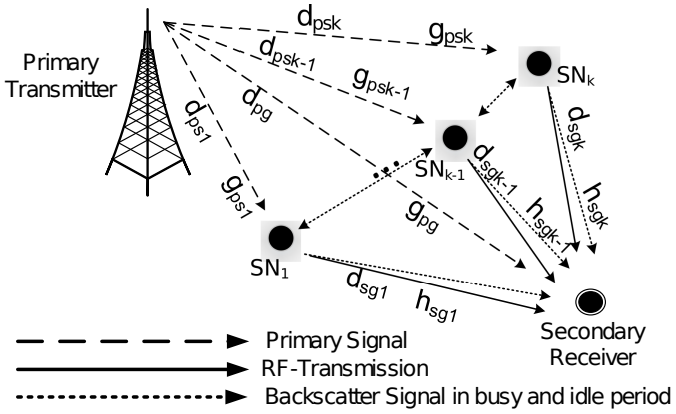

Fig. 1: System model (during busy and idle period).

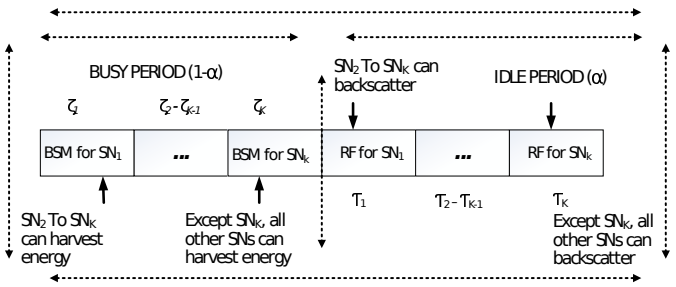

Fig. 2: The overall transmission time frame of the considered CRN.

A. Mode Selection During Busy Period

In our proposed setup, during a busy period, the SNs can either recharge their batteries by harvesting primary signals or choose the backscattering mode to transmit their data. More specifically, the whole busy period is divided into sub-slots such that each SN gets an opportunity to backscatter its data to the gateway to operate in BSM while all other SNs operate in EHM. Precisely, during busy periods, the received primary signal at SN_k can be expressed as

$$Y_k = \frac{T_p |g_{ps_k}|^2 x_1}{\left(1 + d_{ps}\right)^{\gamma}} + n_k, \tag{1}$$

where as T_p is the transmit power of PT, x_1 is the information signal, γ is the path loss exponent, and n_k is the receiver noise introduced at k^{th} SN. The total amount of energy harvested by k^{th} SN during an idle period can be expressed as

$$HE_k = (1 - \alpha - \zeta_k) E_k, \tag{2}$$

where $E_k = \frac{\eta T_p |g_{ps}|^2}{(1+d_{ps})^{\gamma}}$ and η is the energy conversion efficiency.

During a busy period, the k^{th} SN operates in BSM for ζ_k time when all other nodes operate in EHM. The SN_k backscatter the signals received from the PT towards the SR. The throughput of SN_k operating in BSM for ζ_k time during a busy period can be calculated as:

$$U_k^B = \zeta_k B_k^{BB}, \tag{3}$$

here B_k^{BB} represents the backscatter transmission rate. Note that for total K SNs, the overall busy period is equally divided using TDMA, and the total backscattering time does not exceed the busy period, i.e., $(\zeta_k < 1 - \alpha)$.

B. Mode Selection During Idle Period

In our proposed scheme, SNs adopt two different modes of communication during the idle period, i.e., RF transmission mode (RFTM) and BSM. The proposed approach is different from [11], where SNs during the idle period only operate in RFTM. More specifically, in our proposed scheme, a k^{th} SN operates in RFTM for τ_k duration of idle time α and operates in BSM for the rest of the $(\alpha - \tau_k)$ time. To perform backscatter communication during idle time, the SNs exploit the RF signals of the nodes operating in RFTM. Precisely, for each τ_k time when the k^{th} SN is operating in RFTM, the $K-1$ SNs utilise the RF signals to perform backscatter operation. The achievable throughput of k^{th} SN while operating in RFTM and BSM can respectively be calculated as

$$U_k^h = \omega_k \tau_k W log_2 \left(1 + \frac{S_k}{P_k^o}\right), \tag{4}$$

$$U_k^h = (\alpha - \tau_k) B_k^{BI}, \tag{5}$$

where $S_k = \frac{HE_k}{\tau_k}$, is the transmit power of k^{th} SN, ω_k is the transmission efficiency during the idle period, W is the primary channel bandwidth, and P_k^o is the ratio between noise power and channel gain (σ/h_{sg}), respectively. Likewise, in (5) $(\alpha - \tau_k)$ is the backscattering time of the k^{th} SN and B_k^{BI} is the backscattering rate during the idle period.

C. Sum-Rate Optimisation

The overall throughput achieved by a k^{th} SN in both busy and idle periods can be expressed as

$$U_k = U_k^B + U_k^h + U_k^I. \tag{6}$$

Likewise, in this paper, the term sum-rate is defined as the overall throughput achieved by the network during both busy and idle periods. Mathematically,

$$U_{overall} = \sum_{k=1}^{K} U_k = \sum_{k=1}^{K} (U_k^B + U_k^h + U_k^I). \tag{7}$$

Note that for (7), in order to be valid, it must ensure that the total backscattering time does not exceed the overall busy period $\left(i.e., \sum_{k=1}^{K} \zeta_k \leq 1 - \alpha\right)$ and combined RF transmission time of all SNs must not exceed the total idle period $\left(\sum_{k=1}^{K} \tau_k \leq \alpha\right)$.

1) Optimization Problem: The optimisation problem, which aims to maximise the overall network sum-rate, can be formulated as

$$(\mathbf{P}_1) \max_{\zeta, \tau} \left(U_{overall}\right)$$
$$\text{subject to} \begin{cases} \sum_{k=1}^{K} \zeta_k \leq 1 - \alpha, \\ \sum_{k=1}^{K} \tau_k \leq \alpha, \\ \zeta_k, \tau_k \geq 0, \forall k \in \mathbb{K} \end{cases} \tag{8}$$

The first constraint in (8) guarantees that the total backscattering times of all SN_k will be less than equal to the busy period. Likewise, the second constraint ensures that the total transmit times of all SN_k will be less than equal to the idle period. Furthermore, the third constraint clarifies that the lower bonds of the corresponding variables are equal to zero. To prove the concavity of $U_{overall}$ w.r.t. ζ_k and τ_k, we examine the second-order partial derivatives of each throughput. $U_{overall} = \sum_{k=1}^{K} \left(U_k^B + U_k^h + U_k^I\right)$ is a sum of individual SN throughput functions, where U_k^B and U_k^I are linear in ζ_k and τ_k, and thus inherently concave. U_k^h is fundamentally concave due to its logarithmic nature. This assumes all parameters, including ω_k, W, and η, are positive. A detailed proof of the problem's convexity is provided in Appendix 1. Here, the optimization problem is solved using the interior point method under some imposed constraints to maximise the overall secondary network throughput, and the QoS requirements are satisfied for individual secondary nodes. With the proposed scheme, optimal values (of ζ and τ) are obtained by solving (8).

III. NUMERICAL RESULTS AND DISCUSSIONS

Numerical values of the transmit power of PT, primary channel idle period, EH efficiency, transmission efficiency and

TABLE I: Simulation Parameters and Their Values

Parameters	**Studied Values**
Primary channel idle period (α)	0.3
Transmission power $PT(T_k^{tp})$	17kW
Backscatter transmission rate (B_k^{BB})	25kbps
Energy Harvesting Efficiency (η)	0.8
Transmission Efficiency (ω)	0.8

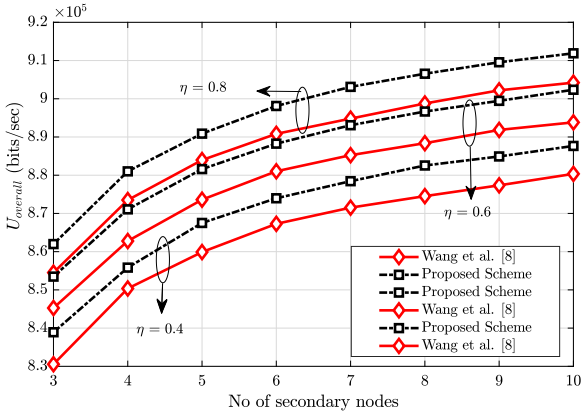

Fig. 3: Maximum achievable throughput of the network by using optimal values of zeta and tau for every individual node. Where no. of SNs = 3-10, $B_k^{BB} = 25kbps$, $\alpha = 0.3$ and $\omega = 0.8$.

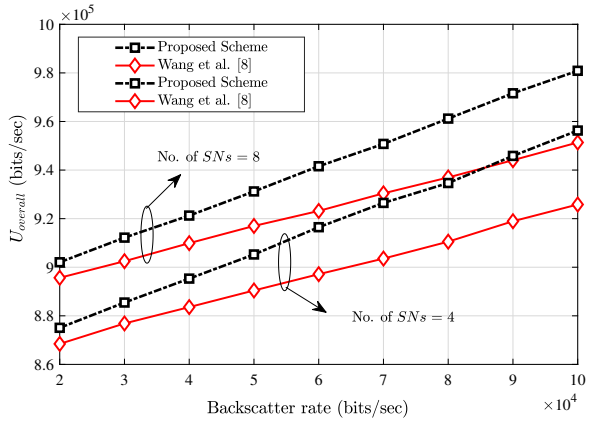

Fig. 4: Optimal analysis of secondary network sum-rate with varying backscatter rate. Where $B_k^{BB} = 20 - 10kbps$, $\alpha = 0.3$, $\eta = 0.8$ and $\omega = 0.8$.

backscatter transmission rate are mentioned in Table 1. The bandwidth and frequency of the signal are 100 kHz and 100 MHz, respectively. The channel between PT to SN_k and SN_k to the gateway is considered as Rayleigh fading, and gain is random for every secondary node. The distance from PT to SN_k is about 2km, and from SN_k to the gateway, it is set as 1 meter. Path loss exponent in urban area cellular radio is 2.7dB. The proposed and legacy schemes' performance analyses are compared, and the optimised simulated results are evaluated in terms of EH efficiency and throughput with varying values of backscatter rate and channel idle ratio.

Fig. 3 evaluates the performance of the secondary system with the increasing number of nodes plus with the varying value of EH efficiency, i.e. $40\%, 60\% and 80\%$ as shown in the resulting graph. When the number of secondary nodes increases, sum-rate also increases (see(11)). The increase in the throughput is because, in this proposed scheme, optimal time allocation is adopted between BSM, EHM and RFM during busy and idle periods, i.e. during busy periods, the secondary nodes either perform EH or backscatter communication subsequently and during idle periods if one of the nodes performs RF communication rest of them adopt backscatter communication this significantly increases the performance of the secondary network sum-rate and that outperforms when compared with wang et al. [11]. The sum-rate also increases when we increase the EH efficiency value (see(2)); this is because by increasing the value of EH efficiency, the nodes store more energy and use that harvested energy for RF communication in the future. So, the achievable throughput performance of the network increases dramatically.

Fig.4 plots the performance of the secondary network by varying the backscattering rate from 20-100kbps and keeping the number of secondary nodes fixed; we achieve improved throughput by increasing the backscatter rate (see(4)). This is because the backscatter transmission rate is increased from 20-100kbps. For instance, before, the nodes were performing

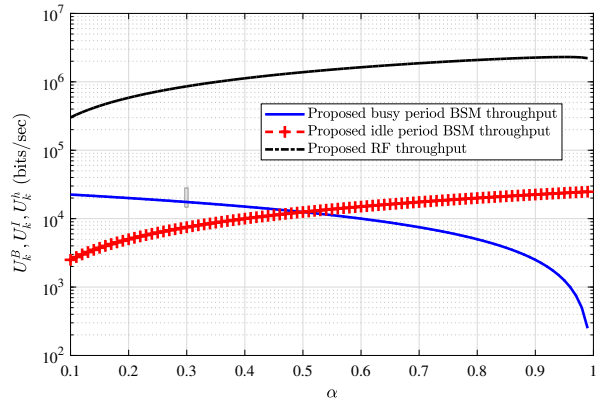

Fig. 5: Secondary network performance for the proposed scheme with varying channel idle ratio. Where no. of SNs = 8, $B_k^{BB} = 25kbps$, $\eta = 0.8$ and $\omega = 0.8$.

backscatter communication with the rate of 20kbps in 0.3 backscatter time, and now the same nodes are using increased rates, so the nodes are able to backscatter more than before due to the improved transmission rates. The performance of the secondary system increases, and the proposed solution gives better results than Wang et al. [11].

Fig. 5 illustrates the maximum throughput for different values of channel idle ratio. This figure depicts the change in the idle channel ratio, which greatly affects the communication modes. This is because if the channel idle ratio is equal to 0.1, the nodes have more chance to store energy or backscatter during the busy period, but the harvested energy cannot be used for RF communication because of a limited idle period. We achieve maximum RF and backscatter communication value when the idle channel increases but lowers in EH and backscatter communication due to a decrease in the channel's busy period.

IV. Conclusion

In this proposed study, we considered an ambient backscatter-enabled, energy-constrained cognitive radio network to optimise scarce resources by introducing a secondary network to utilise the primary network efficiently. We formulated an optimisation problem using an optimal trade-off scheme among BSM, EHM, and RFM during the idle and busy periods of the primary network. The optimal time allocation mechanism is evaluated among multiple users in terms of sum rate, backscatter rate, channel idle ratio, and EH efficiency. The simulated results depict the suggested method outperforming the legacy scheme.

Appendix 1

To prove that $U_{overall}$ is a concave function with respect to the decision variables ζ_k and τ_k, we analyse the second-order partial derivatives of each U_k and the conditions for concavity. The objective function $U_{overall} = \sum_{k=1}^{K} \left(U_k^B + U_k^h + U_k^I\right)$ is a sum of individual SN throughput functions, where U_k^B and U_k^I are linear with respect to ζ_k and τ_k, and thus inherently concave as their second derivatives are zero. The term U_k^h, characterised by a logarithmic function, is fundamentally concave. This analysis assumes that all parameters, including ω_k, W, and η, are positive, ensuring the domain of the logarithmic function remains positive and thus concave.

For a comprehensive understanding of U_k^h's concavity, we delve into its second-order derivatives with respect to τ_k, which are derived as follows:

$$\frac{\partial U_k^h}{\partial \tau_k} = \omega_k W \log_2\left(1 + \frac{S_k}{P_k^o}\right) + \omega_k \tau_k W \frac{1}{\ln(2)\left(1 + \frac{S_k}{P_k^o}\right)} \left(-\frac{S_k}{\tau_k^2 P_k^o}\right).$$

This yields a second derivative with respect to τ_k that is negative, thus confirming U_k^h's concavity in terms of τ_k:

$$\frac{\partial^2 U_k^h}{\partial \tau_k^2} = \frac{-\omega_k W}{\ln(2)\tau_k^2 \left(1 + \frac{S_k}{P_k^o}\right)^2} \left(\frac{S_k}{P_k^o}\right).$$

The indirect dependence of S_k on ζ_k through harvested energy HE_k suggests a similar concavity with respect to ζ_k, albeit not explicitly calculated here, the logical progression and effects on S_k imply this concavity.

Further substantiation of the concavity of U_k^h and consequently U_{overall} leverages the Hessian matrix H composed of the second-order partial derivatives concerning ζ_k and τ_k. The Hessian matrix for U_k^h is structured as:

$$H = \begin{bmatrix} \frac{\partial^2 U_k^h}{\partial \zeta_k^2} & \frac{\partial^2 U_k^h}{\partial \zeta_k \partial \tau_k} \\ \frac{\partial^2 U_k^h}{\partial \tau_k \partial \zeta_k} & \frac{\partial^2 U_k^h}{\partial \tau_k^2} \end{bmatrix}.$$

Given the inherently concave nature of the logarithmic component within U_k^h, alongside the linear (and therefore concave) nature of U_k^B and U_k^I, the Hessian matrix's entries associated with the second derivatives are non-positive. This ensures the Hessian's negative semidefiniteness, a critical condition affirming U_k^h, and by extension U_{overall}'s concavity with respect to ζ_k and τ_k. Accordingly, the formulated optimisation problem to maximise U_{overall} subject to given constraints is recognised as a convex optimisation problem, enabling the application of standard convex optimisation techniques to ascertain the global optimum efficiently.

Acknowledgment

This work was supported by EPSRC projects, CHEDDAR EP/X040518/1 and CHEDDAR Uplift EP/Y037421/1.

References

[1] EricssonInc., "Ceo to shareholders: 50 billion connections 2020," http://www.ericsson.com/thecompany/press/releases/2010/04/1403231, Stockholm, Sweden, 2010, [Online; accessed 2020].

[2] B. Lyu, H. Guo, Z. Yang, and G. Gui, "Throughput maximization for hybrid backscatter assisted cognitive wireless powered radio networks," *IEEE Internet of Things Journal*, vol. 5, no. 3, pp. 2015–2024, 2018.

[3] W. Wang, D. T. Hoang, D. Niyato, P. Wang, and D. I. Kim, "Stackelberg game for distributed time scheduling in rf-powered backscatter cognitive radio networks," *IEEE Transactions on Wireless Communications*, vol. 17, no. 8, pp. 5606–5622, 2018.

[4] A. N. Parks, A. Liu, S. Gollakota, and J. R. Smith, "Turbocharging ambient backscatter communication," in *Proc. ACM SIGCOMM*, Chicago, IL, USA, Aug. 2014, pp. 619–630.

[5] S. T. Shah, K. W. Choi, T. J. Lee, and M. Y. Chung, "Outage probability and throughput analysis of swipt enabled cognitive relay network with ambient backscatter," *IEEE Internet of Things Journal*, vol. 5, no. 4, pp. 3198–3208, Aug. 2018.

[6] D. T. Hoang, D. Niyato, P. Wang, D. I. Kim, and L. B. Le, "Overlay rf-powered backscatter cognitive radio networks: A game theoretic approach," in *2017 IEEE International Conference on Communications (ICC)*, 2017, pp. 1–6.

[7] V. Liu, A. Parks, V. Talla, S. Gollakota, D. Wetherall, and J. R. Smith, "Ambient backscatter: wireless communication out of thin air," *ACM SIGCOMM Computer Communication Review*, vol. 43, pp. 39–50, 2013.

[8] H. D. Thai, D. Niyato, P. Wang, D. I. Kim, and Z. Han, "The tradeoff analysis in rf-powered backscatter cognitive radio networks," in *2016 IEEE Global Communications Conference (GLOBECOM)*, 2016, pp. 1–6.

[9] S. T. Shah, K. W. Choi, S. F. Hasan, and M. Y. Chung, "Throughput analysis of two-way relay networks with wireless energy harvesting capabilities," *Ad Hoc Networks*, vol. 53, pp. 123–131, 2016.

[10] S. Gong, X. Huang, J. Xu, W. Liu, P. Wang, and D. Niyato, "Backscatter relay communications powered by wireless energy beamforming," *IEEE Transactions on Communications*, vol. 66, no. 7, pp. 3187–3200, 2018.

[11] D. T. Hoang, D. Niyato, P. Wang, and D. I. Kim, "Optimal time sharing in rf-powered backscatter cognitive radio networks," in *2017 IEEE International Conference on Communications (ICC)*, 2017, pp. 1–6.

[12] S. T. Shah, D. Munir, M. Y. Chung, and K. W. Choi, "Information processing and wireless energy harvesting in two-way amplify-and-forward relay networks," in *2016 IEEE 83rd Vehicular Technology Conference (VTC Spring)*, 2016, pp. 1–5.

[13] A. Iqbal and T.-J. Lee, "Opportunistic backscatter communication protocol underlying energy harvesting iot networks," *IEEE Access*, vol. 11, pp. 89 568–89 580, 2023.

[14] B. Gu, D. Li, Y. Xu, C. Li, and S. Sun, "Many a little makes a mickle: Probing backscattering energy recycling for backscatter communications," *IEEE Transactions on Vehicular Technology*, vol. 72, no. 1, pp. 1343–1348, 2023.

[15] R. Nesbitt, S. T. Shah, M. Wagih, M. A. Imran, Q. H. Abbasi, and S. Ansari, "Next-generation iot: Harnessing ai for enhanced localization and energy harvesting in backscatter communications," *Electronics*, vol. 12, no. 24, 2023. [Online]. Available: https://www.mdpi.com/2079-9292/12/24/5020

[16] K. G. Omeke, M. Mollel, S. T. Shah, L. Zhang, Q. H. Abbasi, and M. A. Imran, "Toward a sustainable internet of underwater things based on auvs, swipt, and reinforcement learning," *IEEE Internet of Things Journal*, vol. 11, no. 5, pp. 7640–7651, 2024.